Colloid Polym Sci 275:449–457 (1997)

ORIGINAL CONTRIBUTION

T.Z. Ivanova
I. Panaiotov
F. Boury
J.E. Proust
R. Verger

Enzymatic hydrolysis of poly(D, L-lactide) spread monolayers by cutinase

Received: 19 August 1996
Accepted: 13 December 1996

T.Z. Ivanova · Dr. I. Panaiotov (✉)
Biophysical Chemistry Laboratory
University of Sofia
J. Bourchier str. 1
1126 Sofia, Bulgaria

F. Boury · J.E. Proust
Pharmacie Galénique
et Biophysique Pharmaceutique
Faculté de Pharmacie
16 Bd Daviers
49100 Angers, France

R. Verger
ERS 26 "Lypolyse enzymatique" du Centre
National de la Recherche Scientifique
B.P. 71
13402 Marseille Cedex 9, France

Abstract The enzymatic hydrolysis of a model poly(D, L-lactide) by cutinase was studied by using a barostat surface balance. A theoretical approach based on the adaptation of the Michaelis–Menten scheme at the interface and a process of random fragmentation of the macromolecules was developed. The role of the interfacial organisation of the reaction products was discussed. Hydrolysis rate constant values and the specific activity were estimated and compared with those obtained for the hydrolysis of lipid monolayers.

The process of fragmentation of the interfacial polymer structures was visualised by using AFM imaging.

Key words Poly(D, L-lactide) – spread monolayer – enzymatic hydrolysis – cutinase

Introduction

The microparticles of poly(D, L-lactide) (PLA 50) and related polymers are often used as delivery device for controlled drug release [1–4]. *In vivo*, the polyester matrix containing drug undergoes a chemical hydrolysis and scission of ester bonds, leading to the appearance of water-soluble polymer fragments, progressive erosion and degradation of the particles and drug release. The end-products of the degradation process are totally bioresorbable by metabolization.

Many physicochemical processes are involved in the processes of progressive degradation of microparticles with complex structure and the drug release. The role of the various degradation factors was intensively studied *in vivo* and *in vitro* [1–14]. Attention was paid particularly to the eventual role of the hydrolytic enzymes (carboxylic esterase, α-chymotrypsin, etc.) on the degradation process [6, 9]. Because of the complexity of the phenomenon, the discussion in the literature is largely intuitive [14]. Recently, a quantitative theoretical and experimental analysis of the most important step of the degradation process – the hydrolysis and scission of ester bonds of simply organized model polyester structures was proposed [15, 16]. A dilute polymer molecular solution is probably the simplest model system. In [15] the acid-catalysed hydrolysis of PLA in solution is followed by analysing the ^{1}H-NMR spectra taken during the kinetics. Random scission and chain-end scission mode of hydrolysis were tested and the hydrolysis rates of the internal and chain-end ester bonds were estimated.

Colloid & Polymer Science, Vol. 275, No. 5 (1997)

Another suitable model system is a polyester monolayer. In [16] the kinetics of hydrolysis of PLA 50 monolayer spread at basic and acidic pH was followed by using a barostat surface balance. A theoretical approach based on the random fragmentation of polymer molecules leading to appearance of small soluble fragments was developed and the hydrolysis rate constants were determined. The role of the interfacial organization of the reaction products was discussed.

The aim of this paper is the study of the mechanism of enzymatic hydrolysis of PLA 50 monolayer spread at the air–water interface. As a model hydrolytic enzyme, a purified recombinant cutinase from *Fusarium solani* was chosen. The reason for such choice is motivated by the fact that the natural substrates of cutinase are ubiquitous biopolyesters (i.e., cutin) protecting the surface of leaves, fruits, etc., and which can have homologous properties with PLA. The course of the enzymatic interfacial hydrolysis leading to the appearance of water-soluble oligomers can be followed by using a traditional barostat surface balance. The interfacial organization of the ester groups can be controlled and modified easily by variation of the surface density and the surface pressure.

Materials and methods

Materials

The PLA 50, a poly(D, L-lactic acid) stereocopolymer (Fig. 1) was obtained from CRBPA (Montpellier, France). According to the Vert classification [17] it contains 50% of L-repeating units. Its mean molecular weight (M_w) determined by size-exclusion chromatography was 41 600. A mean number of polymerization $n_p = 578$ can be calculated. Nevertheless, the polymolecularity index was kept in the range 1.6–1.9.

The purified recombinant cutinase was a gift from Dr. G. Matthyssens, CORVAS International N.V. (Gent, Belgium). This preparation was in the form of lyophilized powder at more than 95% purity (w/w). The specific activity of cutinase towards various substrates is: triolein – 800 U/mg, *p*-nitrophenylbutirate – 2000 U/mg and tributirine – 4000 U/mg [18].

Tris used in the buffer solution was purchased from Merck. Dichloromethane (DCM) and HCl were supplied by Prolabo (Paris-France) and used without further purification Double distilled water was used.

Fig. 1 Formula of poly(D, L-lactic acid) stereocoplymer (PLA 50)

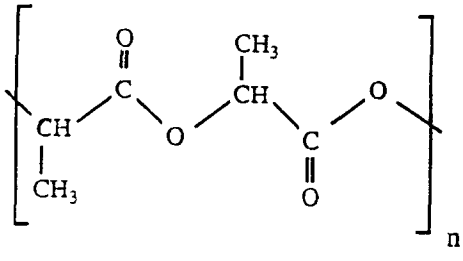

Measurements at the air/water interface

The decrease of the surface area (ΔA) versus time (t) at constant surface pressure (π) was measured during the interfacial hydrolysis of the PLA 50 monolayer. An automatic barostat surface balance KSV 2200 (Finland) with a "zero order" trough [19] composed of a reaction compartment at pH = 9 (buffer solution 5 mM Tris–HCl) (volume 50 cm^3, surface area 50 cm^2) and a reservoir compartment at pH = 6.8 (pure water) (surface area 290 cm^2) communicating by means of narrow surface canal (Fig. 2) was used.

The PLA 50 monolayer was spread from volatile DCM solution (c = 1 mg/ml) by using an Exmire microsyringe. After spreading on the all maximum available area (340 cm^2) of KSV surface balance, the PLA 50 monolayers were compressed with constant velocity U_b = 100 $cm^2\ min^{-1}$ until a given value of the surface pressure.

Fig. 2 Schematic representation of the "zero order" trough of the barostat surface balance [19] composed of a reaction compartment at pH = 9 containing cutinase and a reservoir compartment at pH neutral communicating by means of a narrow surface canal

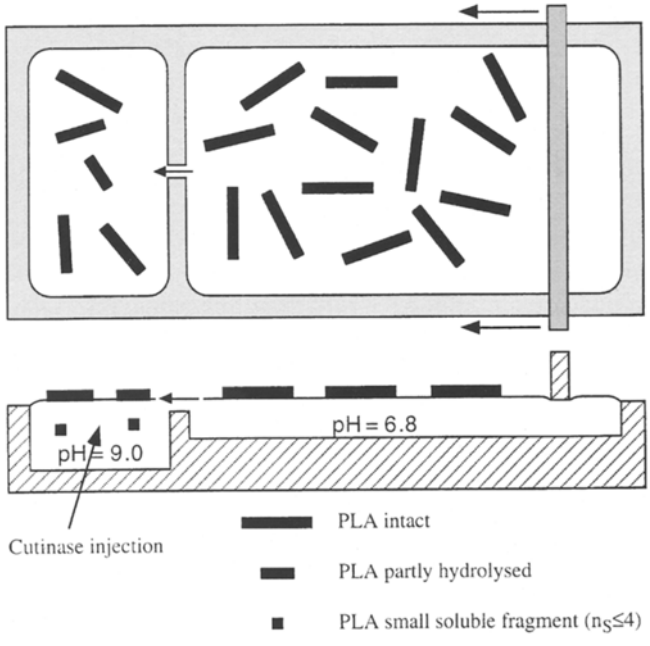

The barostat system was then set on and the cutinase injected into the reaction compartment. In order to homogenize the cutinase solution, the bulk of the reaction compartment was stirred continuously with a magnetic rod at 250 min^{-1}.

Atomic force microscopy

After LB transfer on a freshly cleaved mica plate, we carried out AFM imaging in the contact mode with a commerical instrument (Autoprobe CP, Park Scientific Instruments) fitted with a 0.6 μm cantilever and a monocristalline tip.

Results and discussion

The dynamical isotherm surface pressure (π) - area per lactic unit (A) of PLA 50 monolayer spread on pure water (Fig. 3) was previously analysed [20–22]. The inflection point at about $\pi = 10\ mN\,m^{-1}$ and $A = 17\ Å^2$ per monomer, corresponds to a closely packing of all lactic segments at the surface in accordance with the area occupied by one lactic unit. The flat plateau at $\pi = 15.6\ mN\,m^{-1}$ was interpreted as a phase transition and formation into the air adjacent phase of the tridimensional structures (loops) organised in microdomains.

The decrease of the surface area (ΔA) with time (t) recorded at various constant surface pressure (π) during the interfacial hydrolysis after injection of cutinase into the reaction compartment is presented in Fig. 4. A typical sigmoid shape of curves with a period of latency is observed. The $\Delta A(t)$ curves change monotonously with the increase of the surface pressure until the phase transition.

Fig. 3 Surface pressure (π) – area per lactic unit (A) isotherm of PLA 50 monolayer spread on aqueous subphase. The arrow shows the state, observed in AFM imaging (see Fig. 9)

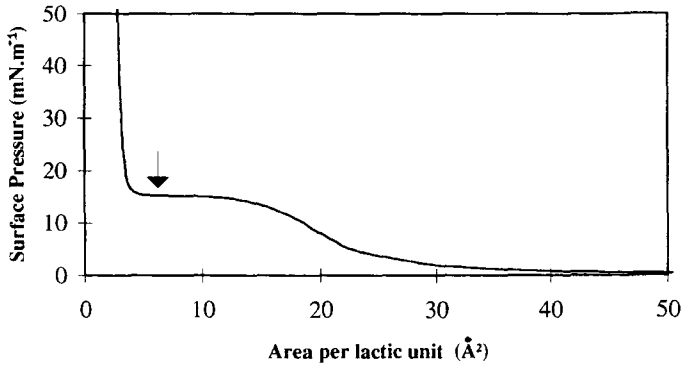

At $\pi = 16\ mN\,m^{-1}$ in the plateau of transition it is quasi-impossible to follow the hydrolysis.

The dependence of the kinetic curves $\Delta A(t)$ on the enzyme concentration (E_0) in the subphase is measured at constant surface pressure $\pi = 10\ mN\,m^{-1}$ corresponding to a closely packing of all lactic segments at the surface (Fig. 5). The observed effects increase with the enzyme concentration.

The course of the interfacial hydrolysis can be described using the adaptation of the Michaelis–Menten kinetic scheme, proposed by Verger [23, 24] (Fig. 6). The model consists of two successive steps. The first one is a reversible penetration of a water-soluble enzyme E into the interfacial layer of substrate molecules S. The penetration step, leading to a more favourable energetic state of the enzyme E^* is followed by a two-dimensional Michaelis–Menten kinetic scheme. The enzyme at the interface forms the E^*S complex which is subsequently decomposed.

In the case of the hydrolysis of simple molecules with short hydrocarbon chains, the reaction products P are soluble in the water phase and desorb instantaneously away from the interface. During the hydrolysis in the barostat conditions, each desorbed molecule is supplied instantaneously by the reservoir and the decrease of the surface area ΔA reflects directly the kinetics of product formation $P(t)$. An initial period of latency due to the slow penetration of the enzyme into the film is usually observed until a steady state in the product formation develops. An important detail should be mentioned here: during the hydrolysis in the barostat conditions the number of substrate molecules per unit area S in the reaction compartment is maintained constant.

The adaptation of the Michaelis–Menten scheme to the important case of polymer interfacial hydrolysis can be made as follows. The theoretical analysis of the obtained kinetic curves $\Delta A(t)_\pi$ is based on the supposition that the observed decrease of the area is due to the progressive appearance of soluble small fragments, during the hydrolysis of polyester molecules and their instantaneous solubilization in the aqueous subphase. Then, the observed initial delay in $\Delta A(t)_\pi$ curves is related to the progressive appearance of small soluble fragments during the random fragmentation process in addition to the slow incorporation of the enzyme into the film. The analysis of the general case when the characteristic times of both processes are of the same order of magnitude is a difficult task. We will consider the limiting case when the binding of the enzyme is expected to be faster process.

From the mass balance corresponding to the kinetic scheme of the Fig. 6 it must be fulfilled that

$$S_0 = S + E^*S + P\,, \qquad (1)$$

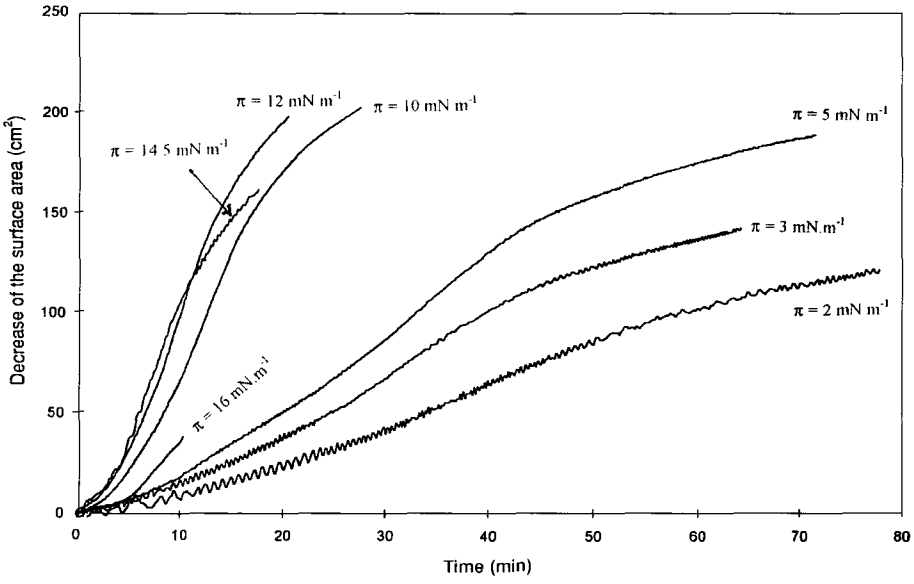

Fig. 4 Decrease of the surface area (ΔA) with time (t) during the enzymatic hydrolysis after injection of cutinase into the reaction compartment at various constant surface pressures: π = 2, 3, 5, 10, 12, 14.5 and 16 mN m^{-1}. The final concentration of cutinase (E_0) was 3 nM

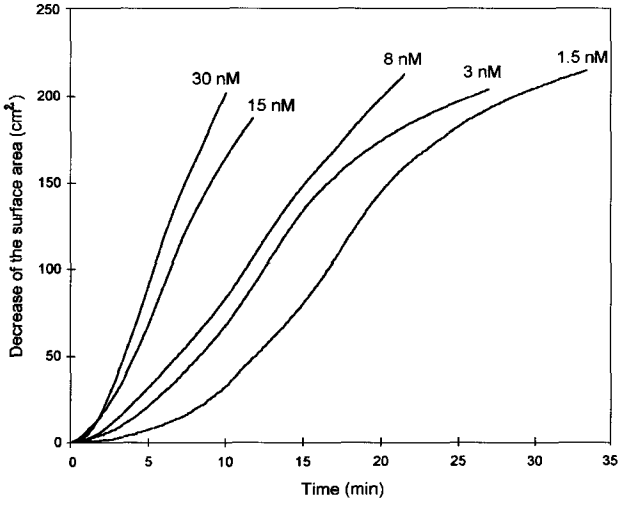

Fig. 5 Decrease of the surface area (ΔA) with time (t) during the enzymatic hydrolysis after injection of cutinase at constant surface pressure π = 10 mN m^{-1} and various enzyme concentration (E_0): 1.5, 3, 8, 15 and 30 nM

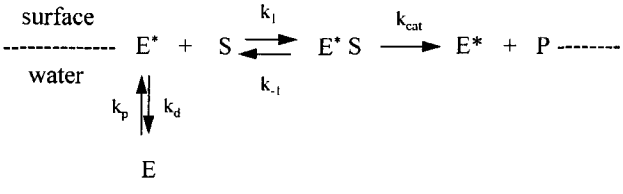

Fig. 6 Adaptation of the Michaelis–Menten scheme describing interfacial catalysis

where S is the number of intact ester groups and P the number of broken ester groups per unit area at any reaction time t, S_0 is the number of intact ester groups at time $t = 0$.

The corresponding kinetic equations are

$$\frac{dE^*S}{dt} = k_1 E_0^* S - (k_{cat} + k_{-1})E^*S \,, \tag{2}$$

$$\frac{dE^*}{dt} = k_p E + (k_{cat} + k_{-1})E^*S - [k_d + k_1 S]E^* \,, \tag{3}$$

$$\frac{dP}{dt} = k_{cat} E^*S \,, \tag{4}$$

$$\frac{dS}{dt} = -k_1 E_0^* S + k_{-1} E^*S \,, \tag{5}$$

$$\frac{dE}{dt} = k_p E - k_d E^* \,, \tag{6}$$

where E^*, S, S_0, E^*S and P are the corresponding surface concentration, expressed as molecules per unit area (molecules cm^{-2}); E is the free enzyme concentration (molecules cm^{-3}).

The corresponding units of the kinetic constants are: k_1 [molecules cm^{-2} s^{-1}]; k_{-1} [s^{-1}]; k_{cat} and k_d [s^{-1}]; k_p [cm s^{-1}].

By addition of Eqs. (2) and (3) we get

$$\frac{dE^*}{dt} + \frac{dE^*S}{dt} = k_p E - k_d E^* \,. \tag{7}$$

We can derivate Eq. (4) with respect to time:

$$\frac{1}{k_{cat}}\frac{d^2P}{dt^2} = \frac{dE^*S}{dt} . \tag{8}$$

By substituting Eqs. (3), (4) and (8) in Eq. (7) together with Eq. (1), the following differential equation is obtained:

$$\frac{d^2P}{dt^2} + [k_{cat} + k_{-1} + k_1 E^*(t)]\frac{dP}{dt}$$

$$- k_1 k_{cat} E^*(t)(S_0 - P) = 0 . \tag{9}$$

The solution of this general equation is rather complicated. The following two usual assumptions can be made. First, we assume that a limited number of all enzyme molecules present in solution has penetrated in the form E^* and E^*S. This assumption is related to the very low values of the ratio interface/bulk and was previously proved [25]. Secondly, we will assume that a stationary state of the enzyme penetration–desorption process is rapidly established [23]. Thus,

$$E \cong E_0 , \tag{10}$$

and

$$k_p E = k_d E^* , \tag{11}$$

where E_0 is the total enzyme concentration expressed in molecules per volume [molecules cm^{-3}].

From Eqs. (10) and (11) we obtain the approximation

$$E^* = \frac{k_p}{k_d} E_0 , \tag{12}$$

and introducing Eq. (12) into Eq. (9)

$$\frac{d^2P}{dt^2} + B\frac{dP}{dt} + CP = CS_0 \tag{13}$$

with

$$B = k_{cat} + k_{-1} + k_1 k_p/k_d E_0 ,$$

$$C = \frac{k_p}{k_d} k_{cat} k_1 E_0 .$$

In the most frequent case of positive and different roots the general solution of Eq. (13) is

$$P = S_0 + Ae^{-kt} + A' e^{-k't} , \tag{14}$$

where

$$k = \frac{1}{2}(k_{cat} + k_{-1})\left\{1 + \frac{Q_m E_0}{k_{cat}} + \sqrt{\left(1 + \frac{Q_m E_0}{k_{cat}}\right)^2 - 4\frac{Q_m E_0}{k_{cat} + k_{-1}}}\right\} , \tag{15a}$$

$$k' = \frac{1}{2}(k_{cat} + k_{-1})\left\{1 + \frac{Q_m E_0}{k_{cat}} - \sqrt{\left(1 + \frac{Q_m E_0}{k_{cat}}\right)^2 - 4\frac{Q_m E_0}{k_{cat} + k_{-1}}}\right\} . \tag{15b}$$

The quantity

$$Q_m \equiv \frac{k_{cat}}{(k_d/k_p) K_m^*} \quad [cm^3 s^{-1} molecule^{-1}]$$

is a global kinetic constant called "interfacial quality" and

$$K_m^* = \frac{k_{cat} + k_{-1}}{k_1} \text{ [molecule cm}^{-2}\text{]}$$

is the interfacial Michaelis–Menten constant [23].

Note that the following relationships are observed:

$$k + k' = (k_{cat} + k_{-1})\left(1 + \frac{Q_m E_0}{k_{cat}}\right) \tag{16a}$$

and

$$kk' = Q_m E_0 (k_{cat} + k_{-1}) . \tag{16b}$$

The coefficients A and A' in Eq. (14) are determined using two initial conditions:

$$t = 0, \quad P = 0 \tag{17a}$$

$$t = 0, \quad \frac{dP}{dt} = k_{cat} E^* S \equiv a , \tag{17b}$$

where the initial rate of product formation a can be estimated experimentally.

From Eqs. (14) and (17a, b) we obtain

$$A + A' = - S_0 , \tag{18a}$$

and

$$kA + k'A' = - a . \tag{18b}$$

From Eqs. (18a) and (18b) we get

$$A = \frac{S_0 k' - a}{k - k'} \tag{19a}$$

and

$$A' = \frac{a - S_0 k}{k - k'} , \tag{19b}$$

and finally for the degree of completion of the hydrolysis $\alpha(t)$ we obtain

$$\alpha(t) = \frac{P}{S_0} = 1 + \frac{S_0 k' - a}{S_0(k - k')} e^{-kt} + \frac{a - S_0 k}{S_0(k - k')} e^{-k't} . \tag{20}$$

Note that from Eq. (20), $\alpha(t = 0) = 0$ and $\alpha(t = \infty) = 1$.

In order to describe the experimental results two consecutive approximations can be used

$$\alpha = \frac{P}{S_0} \cong 1 + \frac{k'}{k - k'} e^{-kt} - \frac{k}{k - k'} e^{-k't} \quad (21)$$

if $a \ll S_0 k$ is fulfilled.

$$\alpha = \frac{P}{S_0} \cong 1 - e^{-k't} \quad (22)$$

if $a \ll S_0 k$ and $k \gg k'$ are fulfilled.

Usually, the initial rate of product formation a (and E^*S at $t = 0$) is near to zero and the simplified equation (21) is fulfilled. In order to use the simplified equation (22) the inequality $k \gg k'$ will be justified in the system under study. Note that from Eqs. (15a, b) $k > k'$. Dividing Eq. (22) by the number of polymer molecules per unit area, the simplified Equation (22) can be rewritten for the number of broken $p(t)$ and intact ester groups $s(t)$ per polymer molecule:

$$\alpha(t) = \frac{p}{s_0} = 1 - e^{-k't} . \quad (23)$$

The simplified kinetic equation (23) must be combined with an equation describing the process of uniform random fragmentation of the PLA 50 linear polymer molecules. With the assumption that the reaction activities of all ester groups of the polymer are equivalent, the number ω_x of segments constituted by x lactic units (obtained during the fragmentation of one polymer molecule with initial number of polymerization n_p) is given by

$$\omega_x(\alpha) = \alpha(1 - \alpha)^{x-1}[2 + (n_p - x - 1)\alpha] . \quad (24)$$

The polymer fragmentation process leads to the formation of large insoluble and small soluble fragments. The progressive appearance of small soluble oligomers constituted by $x \leq x_s$ lactic units seems to be one of the reasons of the observed latent period at the beginning of $\Delta A(t)_\pi$ curves. The fraction (β) of the solubilized lactic units can be easily obtained from Eq. (24):

$$\beta(\alpha) = \frac{\sum_{x=1}^{x_s} \omega_x x}{n_p} . \quad (25)$$

The theoretical prediction $\beta(\alpha)$ assuming $x_s = 4$ [26] and $n_p = 578$ is presented in Fig. 7.

A continuity equation at the interface corresponding to the barostatic conditions in Fig. 2 must be associated with Eqs. (23) and (25). This equation is deduced numerically from the experimental results $\Delta A(t)_\pi$ presented in Figs. 4 and 5. Taking into account the progressive solubilization of polymer molecules initially present in the reaction compartment ($A_{t=0} = 50\ cm^2$) as well as the contribution of

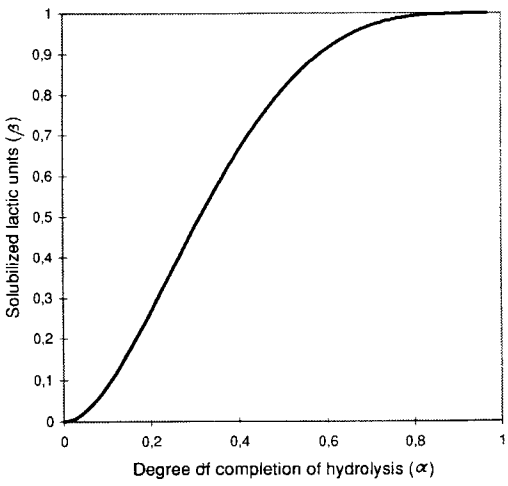

Fig. 7 Fraction of the solubilized lactic units (β) as a function of the degree of completion of hydrolysis (α) calculated from Eq. (25) ($x_s = 4$ and $p = 578$)

the i portions (ΔA_{t-t_i}) of intact polymer molecules supplied progressively by the reservoir to the reaction compartment (see Fig. 2), the following theoretical expression for the surface area decrease is obtained:

$$\Delta A(t) = A_0 \beta(t) + \sum_{i=0}^{i} \Delta A(t_i)\beta(t - t_i) . \quad (26)$$

Using an appropriate numeric procedure the prediction of Eq. (26) together with Eqs. (25), (24) and the simplified equation (23) is fitted with the experimental data $\Delta A(t)$ from Figs. 4 and 5. The values for the chosen fitting parameter k' are calculated. A typical result (points) obtained in this way is compared with the experimental data (curve) in Fig. 8 ($E_0 = 8$ nM; $\pi = 10\ mN\,m^{-1}$; $k' = 0.080 \pm 0.005\ min^{-1}$).

Using Eq. (16b) and the experimental values of Q_m and k_{cat} (see below) the value of k was estimated to be at least one order of magnitude larger than k', i.e., the approximation $k \gg k'$ is justified. It should be noted that the attempt to fit the experimental data with two rate constants ($k \gtrsim k'$) and Eq. (21) (data not shown) leads to worse results: two inflection points in $\Delta A(t)$ curve appear while the experimental curve shows a sigmoid shape with one inflection point.

The theoretical prediction (based on the proposed mechanism of random fragmentation of PLA 50 molecules leading to the production of small soluble fragments) seems to be in good agreement with the experimental results at the beginning of the reaction. In the later stages of the hydrolysis, the course of the reaction is faster in comparison with the theoretical prediction. A progressive enzyme penetration in the monolayer instead of the

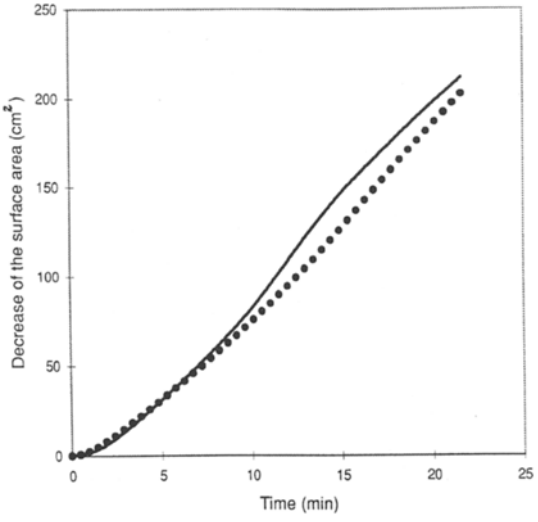

Fig. 8 Decrease of the surface area (ΔA) with time (t) during the enzymatic hydrolysis at $\pi = 10$ mN m^{-1} (—) experimental data from Fig. 5; (●) theoretical prediction of Eqs. (23)-(26) with a fitting parameter $k' = 0.080$ min^{-1}

constant value of E^*, assumed by Eq. (12) could explain the observed hydrolysis acceleration. It was shown [27] that a preferential binding of the cutinase on negatively charged substrates occurs. In our system, the hydrolytic insoluble products charged negatively at pH = 9 are accumulated in the monolayer and an electrostatic attraction can be the reason of the progressive enzyme penetration and the observed discrepancy.

Table 1 Hydrolysis rate constant k' at various surface pressure π (at $E_0 = 3$ nM)

π [mN m^{-1}]	k' [min^{-1}]
3	0.022
5	0.027
10	0.064
12	0.073
14.5	0.084

The obtained values of the hydrolytic rate constant (k') as a function of the surface pressure (π) of the PLA 50 monolayers are shown in Table 1.

Generally speaking, the rate of the reaction depends on the interfacial organization of lactic units from $\pi = 3$ to 10 mN m^{-1} corresponding to maximal close packing of the monolayer, the true hydrolytic rate constant increases with the increase of the number of ester bonds per unit area able to be hydrolysed. At larger surface pressures $\pi = 12$ and 14.5 mN m^{-1}, when the tridimensional structures are present, the observed apparent rate constant takes into account not only the process of the degradation of the polylactic monolayer but also the degradation and rapid respreading of the aggregates.

At $\pi = 16$ mN m^{-1} (see Fig. 4) in the plateau of transition it is quasi-impossible to follow the hydrolysis. The process can be visualized by using AFM imaging. The films were sampled at $\pi = 16$ mN m^{-1} in the phase transition before injection of cutinase into the reaction compartment (A) and after hydrolysis (B). The morphology of the condensed domains of PLA 50 (Fig. 9A) is modified profoundly after hydrolytic process (Fig. 9B). As an example, the overheights of the observed structures in

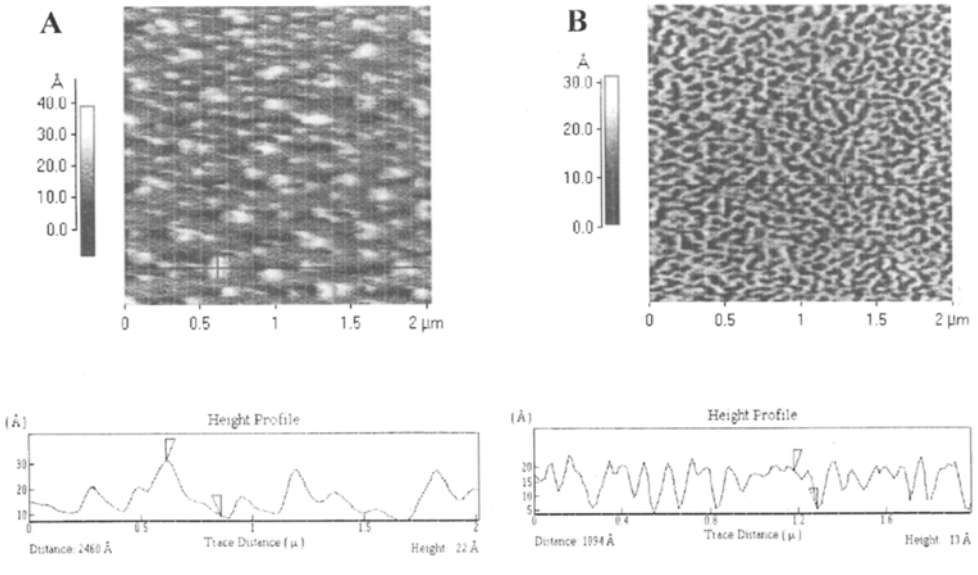

Fig. 9 AFM imaging of PLA 50 LB film sampled in the phase transition ($\pi = 16$ mN m^{-1}) (A) before injection of cutinase into the reaction compartment; (B) after enzymatic hydrolysis

Table 2 Hydrolysis rate constant k' at various enzyme total concentration E_0 (at $\pi = 10\ mN\ m^{-1}$)

E_0 [nM]	k' [min^{-1}]
1.5	0.032
3.0	0.064
8.0	0.080
15.0	0.130
30.0	0.140

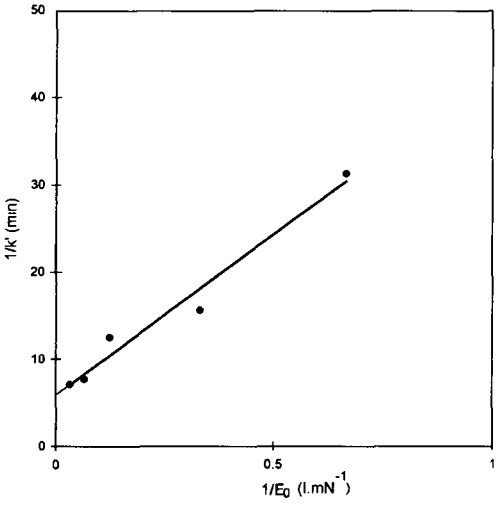

Fig. 10 Dependence of $1/k'$ from $1/E_0$

Fig. 9 decrease from 22 to 13 Å after the hydrolysis. The observed structural modifications are related to the fragmentation and solubilization of the polymer molecules from the monolayer and the aggregates leading to a respreading of the condensed domains.

The hydrolytic rate constant (k') increase with the increase of the enzyme concentration in the subphase (E_0) as shown in Table 2. With the approximation $k \gg k'$ by substituting k from Eq. (16a) into Eq. (16b) the following relationship between k' and E_0 is obtained:

$$\frac{1}{k'} = \frac{1}{k_{cat}} + \frac{1}{Q_m}\frac{1}{E_0}. \qquad (27)$$

In Fig. 10 the data from Table 2 are presented according to the Eq. (27). The values of the global kinetic hydrolysis constant called "interfacial quality" $Q_m = 0.76 \times 10^{-15}\ cm^3\ s^{-1}\ molec^{-1}$ and k_{cat} are estimated (the correlation coefficient is 0.97). By expressing Q_m in more usual units of specific activity (SA) a value of $SA = 0.73 \times 10^{-2}\ mol\ cm^{-2}\ min^{-1}\ M^{-1}$can be compared with the previously obtained value of $SA = 4.2 \times 10^{-2}\ mol\ cm^{-2}\ min^{-1}\ M^{-1}$ for the hydrolysis of 1,3-diolein monolayer by cutinase in presence of an acceptor of lipolytic products [28]. The estimtaed value of $Q_m = 0.76 \times 10^{-15}\ cm^3\ s^{-1}\ molec^{-1}$ can be also compared with the true value $Q_m = 4.1 \times 10^{-15}\ cm^3\ s^{-1}\ molec^{-1}$ obtained for the hydrolysis of DLPC monolayer by phospholipase A_2 [29].

Conclusions

The hydrolysis and scission of ester bonds of polyester macromolecules leading to appearance of water-soluble oligomers are at the origin of the progressive degradation *in vivo* of microparticles fabricated from poly(D, L-lactide).

The study of enzymatic hydrolysis of a model PLA 50 monolayer by cutinase analyses the role of the physicochemical phenomena involved in the reaction (interfacial organization of the reaction products, solubilization of the products, etc.) on the rate and mechanism of the reaction. The developed theoretical approach based on the adaptation of the Michaelis–Menten scheme at the interface and a process of random fragmentation of the polymer molecules allowed us to determine the global rate constant of the enzymatic reaction. The obtained values of the specific activity of cutinase are compared with the previously obtained values for the hydrolysis of monolayers constituted of simple molecules when the reaction products are instantaneously solubilized.

Acknowledgement This work was partially financed by the Bulgarian National Foundation for Scientific Research, by the Bridge-T-lipase Programme of the European Communities under contract BIOT-CT910274 (DTEE) and by BIOTECH G Program BIO-2-CT94-3041. Tz. Ivanova and I. Panaiotov were supported financially by Ministère de l'Education Nationale (France).

References

1. Lewis DD (1990) In: Chasin M, Langer RS (eds) Biodegradable Polymer as Drug Delivery Systems. Marcel Dekker, New York, p 1
2. Vert M (1986) Buck S (eds) CRC Critical Review – Therapeutic Drug Carrier systems, Vol. 2. CRC Press, Boca Raton, p 291
3. Holand SJ, Tighe BJ, Gould PL (1986) J Control Release 4:155
4. Mauduit J, Vert M (1993) STP Pharma Sci 3(3):197
5. Chu CC (1982) J Biomed Mater Res 16:117
6. Makino K, Arakawa M, Kondo T (1985) Chem Pharm Bull 33:1195
7. Makino K, Ohshima H, Kondo T (1986) J Microencapsulation 3:203
8. Coffin MD, McGinity W (1992) Pharm Res 9:200
9. Chu CC, Williams DF (1983) J Biomed Mater Res 17:1029

10. Kaetsu I, Yoshida M, Asano M, Yamanaka H, Imai K, Yuasa H, Mashimo T, Suzuki K, Katakai R, Oya M (1987) J Control Release 6:249
11. Vert M, Li S, Garreau H (1991) J Control Res 16:15
12. Fukuzaki H, Yoshida M, Asano M, Kumakura M, Mashimo T, Yuasa H, Imai K, Yamanaka H (1991) Biomaterials 12:433
13. Spenlehauer G, Vert M, Benoit JP, Boddaert A (1989) Biomaterials 10:557
14. Göpferich A (1996) Biomaterials 17:103
15. Shih C (1995) J Control Release 34:9
16. Ivanova Tz, Panaiotov I, Boury F, Proust JE, Benoit JP, Verger R (in press) Coll Interface Sci B: Biointerfaces, in press
17. Vert M, Christel P, Chabot F, Leray J (1984) In: Hasting G, Wand Ducheyne P (eds) CRC Press, Boca Raton, p 119
18. Lauwereys M, De Geus P, De Meutter J, Stanssen P, Mattyssens G (1991) In: Alberghina L et al (eds) Lipases-Structure, Mechanism and Genetic Engineering, Vol. 16 VCH, Weinheim, p 243
19. Verger R, de Haas G (1973) Chem Phys Lipids 10:127
20. Boury F, Olivier E, Proust JE, Benoit JP (1993 & 1994) J Colloid Interface Sci 160:1; 163:37
21. Boury F, Gulik A, Dedieu JC, Proust JE (1994) Langmuir 10:1654
22. Boury F, Ivanova Tz, Panaiotov I, Proust JE, Bois A, Richou J (1995) J Colloid Interface Sci 169:380 (1995) Langmuir 11:1636
23. Verger R, Mieras MC, de Haas GH (1973) J Biol Chem 248:4023
24. Havsteen BH, Varon Castellanos R, Molina M, Garcia Meseguer JM, Valero E, Garcia-Moreno M (1992) J Theor Biol 157:523
25. Zografi G, Verger R, de Haas GH (1971) Chem Phys Lipids 7:185
26. Vert M, private communication
27. Egmond MR (1996) In: Malcata FX (ed) Engineering of/with Lipases NATO AS I Series E: Applied Scdiences, Vol 317. Kluwer Acad Publ, (Dordrecht, pp 183 and 193
28. Melo E, Ivanova M, Aires-Barros M, Gabral J, Verger R (1995) Biochemistry 34:1615
29. Ivanova M, Ivanova Tz, Verger R, Panaiotov I (1996) Coll Surface B: Bioint 6:9